

Coherent spin manipulations in  $\text{Yb}^{3+}:\text{CaWO}_4$  at  $X$ - and  $W$ -band EPR frequenciesR. M. Rakhmatullin,<sup>1</sup> I. N. Kurkin,<sup>1</sup> G. V. Mamin,<sup>1</sup> S. B. Orlinskii,<sup>1</sup> M. R. Gafurov,<sup>2,\*</sup> E. I. Baibekov,<sup>1</sup> B. Z. Malkin,<sup>1</sup> S. Gambarelli,<sup>3</sup> S. Bertaina,<sup>4</sup> and B. Barbara<sup>5</sup><sup>1</sup>Kazan State University, 420008 Kazan, Russian Federation<sup>2</sup>Centre of Biomolecular Magnetic Resonance, Institute of Physical and Theoretical Chemistry, Max-Von-Laue Str. 7, 60438 Frankfurt, Germany<sup>3</sup>Laboratoire de Chimie Inorganique et Biologique, UMR-E 3 CEA-UJF et FRE CNRS 3200 INAC, CEA-Grenoble, 38054 Grenoble, France<sup>4</sup>IM2NP, CNRS, Universit es Paul C ezanne, Ave. Escadrille Normandie Niemen, Case 142, 13397 Marseille Cedex 20, France<sup>5</sup>Institut N el, CNRS, UJF, BP 166, 38042 Grenoble Cedex 09, France

(Received 15 January 2009; revised manuscript received 30 April 2009; published 20 May 2009)

Coherent spin dynamics of impurity  $\text{Yb}^{3+}$  ions in the  $\text{CaWO}_4$  single crystal has been studied using  $X$ - and  $W$ -band EPR. Rabi oscillations of the sample magnetization with damping times comparable to their period, driven by pulses of the microwave field with duration up to  $5 \mu\text{s}$ , were observed. The largest value of the single-qubit figure of merit ( $\sim 6400$ ) is obtained for the high-field component in the  $^{171}\text{Yb}$   $X$ -band EPR spectrum. The spin-lattice relaxation time of the  $\text{Yb}^{3+}$  ions shortens with the increasing resonance frequency while the phase memory time, in contrast, grows noticeably. Variations of the phase memory times are interpreted in terms of spectral and instantaneous diffusions. The increase of the coherence time at the  $W$  band can be used for the application of rare-earth ions as qubits in quantum computing as it has been proposed recently.

DOI: 10.1103/PhysRevB.79.172408

PACS number(s): 76.30.Kg, 03.67.Lx

Nuclear magnetic resonance (NMR) was the first technique to demonstrate nontrivial quantum algorithms with small numbers of quantum bits (qubits).<sup>1</sup> However, the bulk NMR implementation of quantum computers has scalability limitations arising from low nuclear Zeeman energy. As it was pointed out by Warren,<sup>2</sup> the problem of degradation of the signal in quantum computing experiments with a useful number of qubits may be overcome with the use of high-frequency EPR. In previous work<sup>3</sup> it has been proposed that rare-earth solid-state qubits with large single-qubit figure of merit,  $Q_M$ , may be suitable for scalable quantum information processing at liquid-helium temperatures ( $Q_M$  is the number of coherent single-qubit operations, defined as  $\Omega_R T_M / \pi$ , where  $\Omega_R$  is Rabi frequency and  $T_M$  is the phase memory time). In Ref. 3 Rabi oscillations were studied with the EPR technique at the  $X$ -band frequency in the highly diluted paramagnetic  $\text{CaWO}_4:\text{Er}$  single crystal containing 0.001% of impurity trivalent erbium ions. It has been shown that in this single-ion magnet the coherence time of the bulk magnetization increases with cooling and reaches  $\sim 50 \mu\text{s}$  at the lattice temperature 2.5 K and the corresponding value of  $Q_M$  reaches  $\sim 1400$ . Here we present results of studies of the same host matrix,  $\text{CaWO}_4$ , doped with the ytterbium ions. Due to smaller value of the  $g$ -tensor component  $g_{\parallel}$  in comparison to  $g$  factors of the  $\text{Er}^{3+}$  ion in  $\text{CaWO}_4$ , the  $\text{Yb}^{3+}$  ions have longer phase memory times when the external magnetic field is parallel to the crystal symmetry axis. In particular, multiple spin echoes at the  $X$ -band frequencies were observed in  $\text{CaWO}_4:\text{Yb}^{3+}$  crystals at liquid-helium temperatures in Ref. 4. The purpose of the present study was to determine variations of the phase memory time and the decay time of Rabi oscillations with working frequency increase up to 95 GHz. The electronic spin-lattice relaxation time, that presents an upper limit of the phase memory time, shortens with the increasing resonance frequency. However, the gap between the ground crystal-field state and the first-excited energy level of the  $\text{Yb}^{3+}$  ion in  $\text{CaWO}_4$  [ $\sim 115 \text{ cm}^{-1}$

(Ref. 5)] is essentially larger than in the crystal-field spectrum of the  $\text{Er}^{3+}$  ion [ $19 \text{ cm}^{-1}$  (Ref. 6)], and we have reasons to believe that the phonon relaxation in  $\text{CaWO}_4:\text{Yb}^{3+}$  should not be an obstacle in achieving high values of coherence times.

The  $\text{CaWO}_4$  single crystal doped with the  $\text{Yb}^{3+}$  ions (0.0025 at. %) was chosen as a model system to compare the coherence times in the  $X$  and  $W$  bands. The sample was grown by Czochralski method in Magnetic Resonance Laboratory of Kazan State University by N. A. Karpov. The  $\text{Yb}^{3+}$  ions substitute for the  $\text{Ca}^{2+}$  ions at sites with the  $S_4$  point symmetry and have an anisotropic  $g$  tensor in the ground state [ $g_{\parallel}=1.054$ ,  $g_{\perp}=3.914$  (Ref. 7)]. Measurements of cw and echo-detected EPR, Rabi oscillations, electronic spin-lattice relaxation ( $T_1$ ), and phase memory ( $T_M$ ) times were performed using the Bruker Elexsys E580 ( $X$  band) and E680 ( $W$  band) pulse spectrometers at temperatures 4–6 K in magnetic fields  $\mathbf{B}_0$  declined from the crystal  $c$  axis by some arbitrary angles.

Examples of the EPR spectra of the  $\text{Yb}^{3+}$  ions in  $\text{CaWO}_4$  obtained from the two-pulse echo measurements at  $X$  and  $W$  bands are shown in Fig. 1. The spectra consist of a central line corresponding to even ytterbium isotopes with nuclear spin  $I=0$  and several hyperfine satellites due to odd isotopes  $^{171}\text{Yb}$  (14.4%) and  $^{173}\text{Yb}$  (16.2%), with  $I=1/2$  and  $5/2$ , respectively. The angle  $\theta$  between the crystal  $c$  axis and the magnetic field  $\mathbf{B}_0$  was determined from the measured effective  $g$  factor for the central line [ $g=(g_{\parallel}^2 \cos^2 \theta + g_{\perp}^2 \sin^2 \theta)^{1/2}=2\pi\hbar\nu/\mu_B B_0$ , here  $B_0$  is the resonance magnetic field value at the fixed frequency  $\nu$  and  $\mu_B$  is the Bohr magneton]. Spectral line widths are larger for  $W$  band as compared to  $X$  band signals due to dispersion of  $g$  factors  $g_{\parallel}$  and  $g_{\perp}$  and the angle  $\theta$ .<sup>8</sup> The latter makes the major contribution in a tilted orientation.

Measurements of Rabi oscillations as well as the spin-lattice relaxation and phase memory times were carried out mainly at the most intensive central line of even isotopes, but

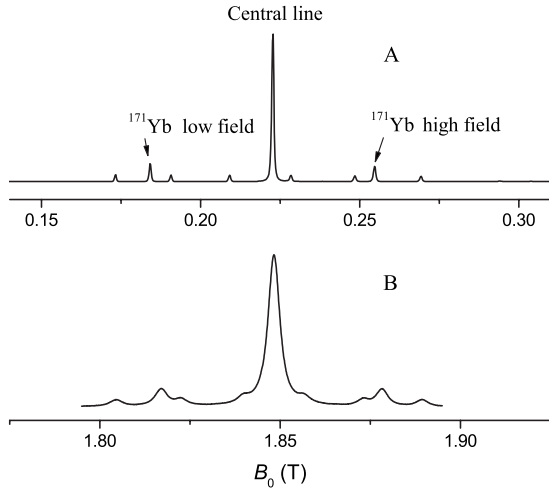


FIG. 1. Two-pulse-echo-detected EPR spectra of the  $\text{Yb}^{3+}$  ions in  $\text{CaWO}_4$  at the resonance frequencies of 9.6634 GHz (A, X band,  $T=10$  K,  $\theta=50^\circ$ ) and 93.9495 GHz (B, W band,  $T=6$  K,  $\theta=67^\circ$ ).

some data were also taken at low- and high-field lines of the  $\text{Yb}^{171}$  isotope. The phase memory times were determined using the two-pulse Hahn echo sequence  $\pi/2-\tau-\pi$ -echo, where the echo amplitude was measured as a function of the time delay  $\tau$  between the pulses. The spin-lattice relaxation times were measured using the pulse sequence *inversion pulse*- $T-\pi/2-\tau-\pi$ -echo, where the time  $T$  was incremented and  $\tau$  was kept fixed. Rabi oscillations were measured using the standard transient nutation technique—after the nutation pulse incrementing in time, with a delay longer than the phase memory time, the  $M(t)$  component of the magnetization parallel to the field  $\mathbf{B}_0$  was detected with a two-pulse echo as a function of the nutation pulse length  $t$ . All experiments were carried out in the microwave magnetic fields  $\mathbf{B}_1$  normal to the plane containing the crystal  $c$  axis and the field  $\mathbf{B}_0$ .

At the X band, the phase memory times were measured using the  $\pi/2$  pulse length of 12 ns for different values of  $\theta$ . The results are collected in Table I. The phase memory time measured at the central EPR line is about 3 orders of magnitude less than the spin-lattice relaxation time and shortens with the increase of  $\theta$ . These results agree well with previous studies of this system (the longest phase memory time was observed when the magnetic field  $B_0$  was parallel to the  $c$  axis<sup>9</sup>).

The inverse coherence time  $T_M$  can be related to the EPR line broadening due to fluctuations of local magnetic fields formed by paramagnetic ions and magnetic nuclei of the host matrix. The magnetic-dipole interactions between the  $\text{Yb}^{3+}$  ions result in the static broadening with the half width  $\Delta\omega_{1/2}^d = \frac{4\pi^2}{9\sqrt{3}}g^2\mu_B^2\hbar^{-1}C$ ,<sup>10</sup> where  $C$  is the concentration of  $\text{Yb}^{3+}$  ions. In the case of the sample  $\text{CaWO}_4:0.0025\%$  Yb studied in this work, the decoherence due to superhyperfine interactions of  $\text{Yb}^{3+}$  ions with magnetic nuclei in the host matrix is negligible [<sup>183</sup>W nuclei with the spin  $I=1/2$  have natural abundance of 14% and small magnetic moments ( $\gamma/2\pi = 1.75$  MHz/T)].

The interactions between the  $\text{Yb}^{3+}$  ions result in two mechanisms of decoherence: spectral diffusion (SD) and instantaneous diffusion (ID).<sup>11</sup> In the case of ID, the fluctuations of local magnetic fields are induced by spin flips caused by  $\pi/2$  and  $\pi$  pulses in the electron-spin-echo experiments. Only the spins with Larmor precession frequencies detuned from the resonance by values of order  $\chi = \frac{g\mu_B B_1}{2\hbar}$  contribute to such fluctuations. For  $\chi/\sigma < 1$  ( $\sigma$  being the inhomogeneous EPR linewidth) the EPR line is only partially excited. The corresponding relaxation rate is given by the expression  $\Gamma_{\text{ID}} = \Delta\omega_{1/2}^d \langle \sin^2 \frac{\theta_2}{2} \rangle$ .<sup>11</sup> Here  $\theta_2$  is the spin nutation angle during the second ( $\pi$ -) pulse and  $\langle \dots \rangle$  denotes averaging over the distribution of the Larmor frequencies of paramagnetic ions.

In the case of SD, the fluctuations of local magnetic fields

TABLE I. The measured spin-lattice relaxation ( $T_1$ ) and phase memory ( $T_M$ ) times, the damping time ( $\tau_R$ ), the period ( $T_R$ ) of the Rabi oscillations, the single-qubit figures of merit ( $Q_M$ ), and the calculated phase memory times ( $T_M^d$ ) for different values of the angle  $\theta$  between the magnetic field and the  $c$  axis in the  $\text{CaWO}_4:\text{Yb}^{3+}$  (0.0025 at. %) single crystal.

Frequency	$\theta$	EPR lines	$T_1$ (ms)	$T_M$ ( $\mu\text{s}$ )	$T_M^d$ ( $\mu\text{s}$ )	$\tau_R$ (ns)	$T_R$ (ns)	$Q_M$	
X band	10°	Central (even isotopes)	13.1	19	24	60	43	884	
		<sup>171</sup> Yb low field	13.7	92	170	56	42	4400	
		<sup>171</sup> Yb high field	10.7	134	150	56	42	6400	
	13°	Central		16	<21	59	41	780	
	20°	Central		10	<14	48	43	465	
			<sup>171</sup> Yb low field	16.9	74	100	49	44	3360
			<sup>171</sup> Yb high field		85	<130	50	46	3700
		71°	Central	12.2	4.1	2.8	42	37	220
	90°	Central	18.5	3.1	2.5	45	45	140	
W band	67°	Central	0.064	13	8.5	340	160	162	
		Central	0.061	14.5	7.5	61	42	690	
	84°	<sup>171</sup> Yb low field	0.059	13.6	10.4	55	41	660	
		<sup>171</sup> Yb high field	0.060	13.7	10.4	63	42	646	

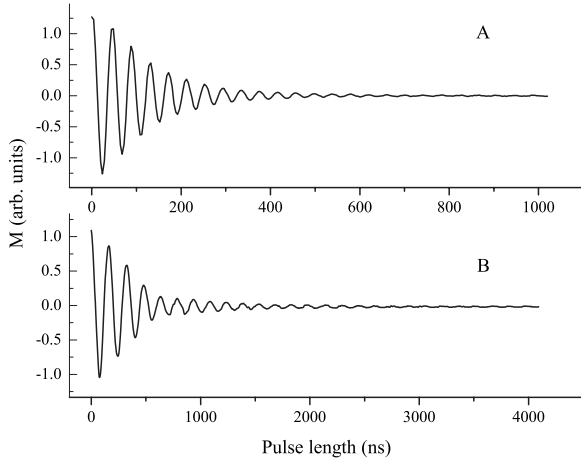


FIG. 2. Rabi oscillations at the central line of the EPR spectrum. (A) X band,  $\theta=50^\circ$ , the number of the observed Rabi oscillations  $N=20$  ( $T_R=44$  ns,  $\tau_R=122$  ns). (B) W band,  $\theta=67^\circ$ ,  $N=27$ .

are induced by spin flips caused by the spin-lattice interaction (the corresponding spin-lattice relaxation rate  $W=1/T_1 \ll \Delta\omega_{1/2}^d$ ) and thus are independent of  $\chi/\sigma$ . Their contribution into  $1/T_M$  can be estimated as  $\Gamma_{SD}=\sqrt{\Delta\omega_{1/2}^d W/2}$ .<sup>11</sup>

At the X band, due to low values of  $W$ ,  $\Gamma_{ID}$  prevails over  $\Gamma_{SD}$ . Since  $\Gamma_{ID}$  is proportional to the number of spins excited by microwave pulses, the calculated phase memory times  $T_M^d=(\Gamma_{ID}+\Gamma_{SD})^{-1}$  for odd Yb isotopes with essentially smaller concentrations (in particular, measured for the high-field and low-field hyperfine components of the  $^{171}\text{Yb}$  spectrum, see Table I) are several times longer than that of even isotopes at the same experimental conditions. The  $T_M^d$  values shorten with the increment of  $\theta$  because the increase of the corresponding effective  $g$  factor results in the increase of  $\Delta\omega_{1/2}^d$  and  $\Gamma_{ID}$ . The calculated values of  $T_M^d$  are presented in Table I, showing good agreement with the experimental data.

The nutation pulse increment for measurements of Rabi oscillations was 4 ns. An example of Rabi oscillations at the X band is presented in Fig. 2(A). The damping oscillations were fitted with the “on-resonance” transient nutation formula

$$M(t) = M(0)\exp(-t/\tau_R)\cos(\Omega_R t), \quad (1)$$

where  $\tau_R$  is the damping time and  $\Omega_R=g_\perp\mu_B B_1/2\hbar$  is Rabi frequency. The values of Rabi frequencies obtained from the Fourier-transformed dependences of the magnetization on the pulse length at different microwave powers  $P$  are proportional to  $\sqrt{P}$  and the relations between the damping time and Rabi frequency (see Fig. 3) were studied by varying simultaneously the amplitudes of the microwave field in the nutation pulse and in the pulses generating echo-signals. It should be noted that, due to the single exponential approximation of decay curves, the relaxation and damping times were determined with relative errors not exceeding 15%.

The obtained values of the single-qubit figure of merit  $Q_M \equiv 2T_M/T_R$  for different declination angles  $\theta$  are in the range of from  $\sim 140$  to 6400. We would like to point out that the optimal sample orientation to get the maximum value of  $T_M$  has not been achieved and one can expect that in the case

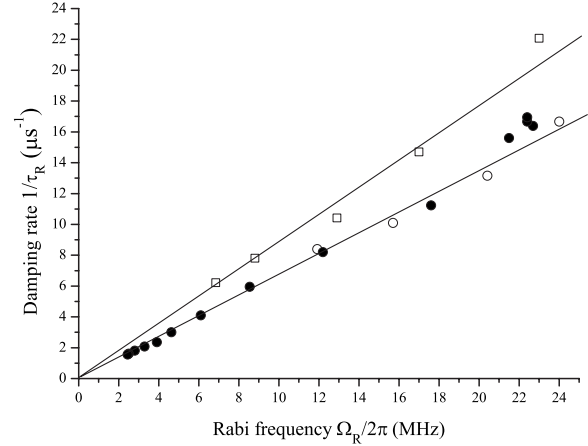


FIG. 3. Damping rates of the Rabi oscillations for the magnetic field  $B_0$  declined from the crystal  $c$  axis by  $90^\circ$  (X band,  $T=4$  K, squares),  $84^\circ$  (W band,  $T=6$  K, filled circles), and  $10^\circ$  (X band,  $T=4$  K, open circles). Solid lines correspond to linear dependences judged by eyes.

of the exact parallel orientation (and smaller concentration of the  $\text{Yb}^{3+}$  ions) the value of  $Q_M$  is several times higher. Assuming the homogeneous distribution of the  $\text{Yb}^{3+}$  ions and the  $^{183}\text{W}$  nuclei, we can roughly estimate the maximum value of  $T_M \sim 500$   $\mu\text{s}$  for a sample with the ytterbium concentration of 0.001 at. % and the corresponding value of  $Q_M$  equals  $\sim 20\,000$ .

Experiments at the W band were carried out in the magnetic fields  $B_0$  declined from the crystal  $c$  axis by  $67^\circ$  and  $84^\circ$  at the temperature 6 K. The lengths of  $\pi/2$  pulses were 32 and 12 ns for  $\theta=67^\circ$  and  $84^\circ$ , respectively. The values of the spin-lattice relaxation and phase memory times were obtained from the fits of the measured echo-decay curves (see Table I). The comparison of the measured spin-lattice relaxation times to data obtained for the same sample at the X band (see also Refs. 12 and 13) confirms that  $T_1$  shortens in accordance with the well-known frequency dependence of the spin-lattice relaxation induced by the one-phonon processes. However, the phase memory times (13–14  $\mu\text{s}$ ) increase noticeably as compared to  $T_M \approx 3\text{--}4$   $\mu\text{s}$ , measured for the close orientations of the magnetic field ( $\theta=71^\circ$  and  $90^\circ$ ) at the X band. The slowing down of the decoherence rate can be explained again in terms of ID and SD processes. Due to an increase of the inhomogeneous line width, the ratio  $\chi/\sigma$  decreases from nearly 1.3 for X band to 0.09 for W band which makes the ID decoherence mechanism ineffective. On the other hand, the  $\Gamma_{SD}$  values increase considerably due to  $T_1$  shortening. Thus, in contrast to the X-band case, the phase relaxation at W band is mostly determined by SD processes. Since SD process is isotope independent, the values of  $T_M$  at W band are approximately the same for even and odd Yb isotopes.

The single-qubit figures of merit at the W band (see Table I) are in the range of the X-band results. However, the value of  $Q_M \sim 690$  ns for  $\theta=84^\circ$  is about 5 times more than  $Q_M$  at the X band for the similar orientation of the magnetic field and the same microwave power. The values of  $T_M$  at W-band frequencies are restricted by the spin-lattice relaxation pro-

cesses which put a limit to get a higher value of the qubit figure of merit.

An example of the measured Rabi oscillations of the magnetization driven by the  $W$ -band radiation is presented in Fig. 2(B). The nutation pulse increment was the same as at the  $X$  band (4 ns). In the magnetic field  $B_0$  declined from the  $c$  axis by  $84^\circ$ , frequencies and damping times of Rabi oscillations were measured for different values of the amplitude of the microwave field  $B_1$  in the nutation pulse (the amplitudes of the microwave field in the detection pulses were kept fixed) and the corresponding variations of  $\tau_R$  with  $\Omega_R$  are presented in Fig. 3.

The study of the damping of the coherent quantum oscillations is a subject of much current interest. It was found experimentally that, at variance to the expected relation  $\tau_R = 2T_M$ , decay rates  $1/\tau_R$  of Rabi oscillations<sup>3</sup> and the transient nutations<sup>14</sup> in the diluted paramagnetic crystals are much higher and depend linearly on Rabi frequency as long as  $\tau_R \ll T_M$ ,

$$\frac{1}{\tau_R} = \frac{1}{2T_M} + \beta\Omega_R. \quad (2)$$

Here the dimensionless coefficient  $\beta$  is the concentration-dependent parameter of the order of  $10^{-1}$ – $10^{-2}$ . Equation (2) was derived in Ref. 15 in the framework of a phenomenological theory based on the assumption that the local magnetic field affecting paramagnetic ions contains a stochastic component proportional to the external microwave field. It is seen in Fig. 3 that the results of our measurements of the damping rate dependence on Rabi frequency for different sample orientations relative to the magnetic field  $B_0$ , for which  $\tau_R \ll T_M$ , do not contradict Eq. (2). At the  $X$  band, the coefficients  $\beta$  vary with the angle  $\theta$  and have values in the range 0.11–0.14 which are comparable to  $\beta \approx 0.05$  corresponding to the data presented in Ref. 3 for Rabi oscillations in the crystal  $\text{CaWO}_4:\text{Er}^{3+}$  with lower concentration of paramagnetic ions. The obtained value 0.11 of the coefficient  $\beta$  for Rabi oscillations induced by the  $W$ -band radiation gives evidence of the universal character of the relation (2) when  $\tau_R \ll T_M$ . In the opposite limit, when  $\tau_R \rightarrow T_M$ , a plateau is

observed in which  $\tau_R$  becomes independent of  $\Omega_R$  and tends to  $T_M$ .<sup>3</sup> The similar dependence of the Rabi oscillations damping time on Rabi frequency was observed in experiments on the impurity  $\text{Cr}^{3+}$  ions in the  $\text{K}_3\text{NbO}_8$  single crystal.<sup>16</sup>

Quantum macroscopic coherent phenomena are widely studied nowadays. Quantum oscillations of the macroscopic magnetization were found in inorganic paramagnetic compounds (see Refs. 3 and 16 and references therein) and very recently in the molecular magnet  $\text{V}_{15}$  (Ref. 17) and the trinuclear iron complex with the  $S=1/2$  ground state.<sup>18</sup> In the present work, the comparable study of Rabi oscillations in the crystal  $\text{CaWO}_4:\text{Yb}^{3+}$  induced by pulses of the  $X$ - and  $W$ -band radiations with durations from several ns up to 5  $\mu\text{s}$  was performed. We have confirmed the prediction of Ref. 3 that the single-qubit figure of merit can be as large as  $10^4$  at liquid-helium temperatures for the rare-earth solid-state qubits based on the entangled electron-nuclear states of Kramers rare-earth ions. It should be noted that the measured low-temperature phase memory times of the  $\text{Er}^{3+}$  and  $\text{Yb}^{3+}$  rare-earth ions diluted in  $\text{CaWO}_4$  are longer by more than 1 order of magnitude than those observed in  $\text{V}_{15}$ , where  $T_M \sim 0.80 \mu\text{s}$ .<sup>17</sup> Similar values were found in more recent experiments on single molecule magnets [ $T_M(\text{Fe}_4)=0.63 \mu\text{s}$ ,<sup>19</sup>  $T_M(\text{Fe}_8)=0.71 \mu\text{s}$  (Ref. 20)]. Finally, the observation of the long-living quantum oscillations of the magnetization induced at the frequency of 94 GHz has demonstrated that the coherence time in highly diluted rare-earth paramagnets can be quite long at the  $W$  band, but one should find a host with the comparatively long spin-lattice relaxation time to consider the rare-earth ion as a feasible qubit in the high-frequency EPR.

This work was supported by the Ministry of Science and Education of the Russian Federation (Project No. RNP.2.1.1.7348), the Russian Foundation for Basic Research (Grant No. 09-02-00930), the Federal Center for Physical and Chemical Research at Kazan State University, and the European Network of Excellence MAGMANet. The authors would like to thank T. Prisner and members of his group (University of Frankfurt, Germany) for providing the possibility to carry out  $X$ -band measurements in their facilities.

\*On leave from Kazan State University.

<sup>1</sup>N. A. Gershenfeld and I. L. Chuang, *Science* **275**, 350 (1997).

<sup>2</sup>W. S. Warren, *Science* **277**, 1688 (1997).

<sup>3</sup>S. Bertaina *et al.*, *Nat. Nanotechnol.* **2**, 39 (2007).

<sup>4</sup>A. Schweiger and G. Jeschke, *Principles of Pulse Electron Paramagnetic Resonance* (Oxford University Press, New York, 2001), pp. 192–193.

<sup>5</sup>G. R. Jones, *J. Chem. Phys.* **47**, 4347 (1967).

<sup>6</sup>E. Bernal G., *J. Chem. Phys.* **55**, 2538 (1971).

<sup>7</sup>J. Kirton and R. C. Newman, *Phys. Lett.* **10**, 277 (1964).

<sup>8</sup>I. N. Kurkin and L. Ya. Shekun, *Fiz. Tverd. Tela (Leningrad)* **9**, 444 (1967) [*Sov. Phys. Solid State* **9**, 339 (1967)].

<sup>9</sup>I. N. Kurkin and V. I. Shlenkin, *Fiz. Tverd. Tela (Leningrad)* **21**,

1469 (1979) [*Sov. Phys. Solid State* **21**, 847 (1979)].

<sup>10</sup>W. B. Mims, *Phys. Rev.* **168**, 370 (1968).

<sup>11</sup>K. M. Salikhov *et al.*, *J. Magn. Reson.* **42**, 255 (1981).

<sup>12</sup>A. A. Antipin *et al.*, *Fiz. Tverd. Tela (Leningrad)* **10**, 1433 (1968) [*Sov. Phys. Solid State* **10**, 1136 (1968)].

<sup>13</sup>A. Kiel and W. B. Mims, *Phys. Rev.* **161**, 386 (1967).

<sup>14</sup>S. Agnello *et al.*, *Phys. Rev. A* **59**, 4087 (1999).

<sup>15</sup>R. N. Shakhmuratov *et al.*, *Phys. Rev. Lett.* **79**, 2963 (1997).

<sup>16</sup>S. Nellutla *et al.*, *Phys. Rev. Lett.* **99**, 137601 (2007).

<sup>17</sup>S. Bertaina *et al.*, *Nature (London)* **453**, 203 (2008).

<sup>18</sup>G. Mitrikas *et al.*, *Phys. Chem. Chem. Phys.* **10**, 743 (2008).

<sup>19</sup>C. Schlegel *et al.*, *Phys. Rev. Lett.* **101**, 147203 (2008).

<sup>20</sup>S. Takahashi *et al.*, *Phys. Rev. Lett.* **102**, 087603 (2009).